horticulturae

MDPI

Article

Fine Mapping and Candidate Gene Validation of Tomato Gene *Carpelloid Stamen and Parthenocarpy* (*CSP*)

Shanshan Li, Kai Wei, Li Zhang, Yu Ning, Feifei Lu, Xiaoxuan Wang, Yanmei Guo, Lei Liu, Xin Li, Can Zhu, Yongchen Du, Junming Li and Zejun Huang *

State Key Laboratory of Vegetable Biobreeding, Institute of Vegetables and Flowers, Chinese Academy of Agricultural Sciences, Beijing 100081, China; 19310462086@163.com (S.L.); 82101209110@caas.cn (K.W.); 82101219106@caas.cn (L.Z.); ny271565853@163.com (Y.N.); 15514907620@163.com (F.L.); wangxiaoxuan@caas.cn (X.W.); guoyanmei@caas.cn (Y.G.); liulei02@caas.cn (L.L.); lixin10@caas.cn (X.L.); zhucan@caas.cn (C.Z.); duyongchen@caas.cn (Y.D.); lijunming@caas.cn (J.L.)
* Correspondence: huangzejun@caas.cn

Abstract: Parthenocarpy and male sterility are highly desirable traits in tomato breeding and molecular study. The stamen carpelloid mutant generally displays male sterility. A natural mutant displaying *carpelloid stamen and parthenocarpy* (*csp*) was identified in our research group. In this study, the *csp* locus was finely mapped to a 65 kb interval, which contained six putative genes. One of them, *Solyc04g081000*, encodes the tomato class B MADS box gene *TAP3* (syn. *SlDEF*). Sequencing data revealed that a *copia* long terminal repeat retrotransposon was inserted in the first intron of the *TAP3* gene of the *csp* mutant. qRT-PCR showed that the expression of *TAP3* was significantly down-regulated in the petals and stamens of the *csp* mutant. A phenotypic analysis of the *TAP3* gene-edited mutants and allelism tests indicated that *TAP3* was the gene underlying *csp*, and *csp* was a novel allelic mutation of *TAP3*. The results of this study will lay the foundation for a further analysis of the function of *TAP3* and provide materials and a basis for a further study of the functional differentiation of tomato B-class genes.

Keywords: tomato; carpelloid stamen; parthenocarpy; fine mapping; candidate gene identification; gene editing

check for updates

Citation: Li, S.; Wei, K.; Zhang, L.; Ning, Y.; Lu, F.; Wang, X.; Guo, Y.; Liu, L.; Li, X.; Zhu, C.; et al. Fine Mapping and Candidate Gene Validation of Tomato Gene *Carpelloid Stamen and Parthenocarpy* (*CSP*). *Horticulturae* **2024**, *10*, 403. https://doi.org/10.3390/horticulturae10040403

Academic Editor: Aisheng Xiong

Received: 11 March 2024
Revised: 6 April 2024
Accepted: 7 April 2024
Published: 16 April 2024

1. Introduction

A carpelloid stamen means that the stamen is transformed into a carpel-like organ [1]. This transformation may result from genetic mutations [2–4] or special environmental conditions [5]. A stamen carpelloid mutant can not only be used to study the genetic basis of floral organ determination, but also serve as a female parent in hybrid seed production due to male sterility [6,7]. Many studies have revealed that mutations in B-class genes are the major cause of the stamen carpelloid mutant [8]. *Arabidopsis* has two B-class genes, *APETALA3* (*AP3*) and *PISTILLATA* (*PI*). Mutants *ap3* and *pi* both exhibit stamen carpelloid [9]. Tomato contains four B-class genes: Tomato *APETALA3* (*TAP3*), *Tomato MADS-box gene 6* (*TM6*), *Solanum lycopersicum GLOBOSA 1* (*SlGLO1*), and *SlGLO2* (also known as Tomato *PISTILLATA*, *TPI*) [10]. Tomato mutants *male sterile-15* (*ms-15*), *ms-26*, *ms-30*, *ms-33*, *ms-47*, *succulent stamens 2* (*sus2*), *stamenless* (*sl*), *sl-2*, and *7B-1* display carpelloid stamens and male sterility. *ms-15*, *ms-26*, and *ms-47* are allelic. There is a single-nucleotide polymorphism (SNP) in the coding region of the *TM6* gene in *ms-15*, which led to a missense mutation (G to W). Additionally, both *ms-26* and *ms-47* have a 12.7 kb deletion, resulting in the absence of the promoter and first four exons of the *TM6* gene [11]. The *sus2* mutant has a single base deletion in the first exon of the *TM6* gene, causing a frameshift and a shortened protein [12]. Regarding the two alleles of *stamenless* (*sl*), *sl-Pr* contains a base pair (bp) deletion in the *TAP3* coding sequence, while *sl-LA0269* has a chromosomal rearrangement in the *TAP3* promoter [13]. A Ds insertion mutant [14] and two EMS mutants [15] of the

TAP3 gene also display carpelloid stamens. It is worth noting that *ms-30*, *ms-33*, *sl-2*, and *7B-1* are allelic and contain sequence variations in the *SlGLO2* gene. Specifically, *ms-30* carries a transversion (G to T) causing a missense mutation (S to I), *ms-33* exhibits a transition (A to T) leading to alternative splicing, and *7B-1* and *sl-2* mutants show the insertion of a retrotransposon approximately 4.8 kb in size [16,17].

Parthenocarpy is a phenomenon in which fruit set and growth occur without the fertilization of ovules. Parthenocarpy is a desirable agricultural trait because it can not only mitigate fruit yield losses caused by environmental stresses but also improve fruit quality by inducing the development of seedless fruit [18,19]. Several natural sources for parthenocarpy in tomato have been identified and characterized, and the genes underlying some of them have been cloned. *Parthenocarpic fruit* (*pat*) encodes an HDIII zip transcription factor called *SlHB1* [20,21]. *Pat-2* encodes a zinc finger–homeodomain (ZHD) protein [22]. *Pat-k* encodes an E-class MADS-box gene, *SlAGAMOUS-LIKE6* (*SLAGL6*) [23]. A parthenocarpic mutant Line 2012 from the EMS-mutagenized M82 cultivar also contains a mutation in the *SlAGL6* gene [24]. *procera* is a putative DELLA mutant [25], while *entire* contains a mutation in *SlAux/IAA9* [26,27]. However, the genes for some parthenocarpic fruit mutants in tomato are still unknown.

Carpelloid stamens and parthenocarpy sometimes occur within the same tomato plant. For example, the *pat* mutant also exhibits carpelloid stamens and exserted ovule-type stamens [28]. *sl-Pr* and *sl-LA0269* develop a variable percentage of parthenocarpic fruits made up of the carpels of whorls 3 and 4, depending on the growing conditions [13]. Furthermore, the parthenocarpic phenotype is observed in two EMS mutant lines of the *TAP3* gene, E7821, and E6483 [15]. Our group found a natural mutant, which displayed *carpelloid stamen and parthenocarpy* (*csp*), from a backcross recombinant inbred line (BIL) derived from a cross between tomato line Heinz1706 and KR2R144. In this study, the *csp* locus was mapped to a 65 kb region on chromosome 4. Sequencing data revealed that the first intron of the *TAP3* gene (*Solyc04g081000*) had a 5 kb retrotransposon insertion, potentially causing *TAP3* to lose function. Additionally, qRT-PCR showed a significant down-regulation of *TAP3* expression in the petals and stamens of the *csp* mutant. A phenotypic analysis of the *TAP3* gene-edited mutants and allelism tests indicated that *TAP3* is the gene responsible for *csp*, and *csp* is a new mutation of *TAP3*. These findings will support a future analysis of *TAP3*'s function and provide materials for studying the differentiation of tomato B-class genes.

2. Materials and Methods

2.1. Plant Materials

csp is a natural mutant that was found in a backcross recombinant inbred line (BIL). The BIL was derived from a cross between the tomato line Heinz1706 (used as recurrent parent) and KR2R144, an inbred line developed by our research group. Its corresponding normal BIL was named wild type (WT). For the genetic analysis and fine mapping of the *csp* locus, an F_2 population consisting of 1162 plants was derived from a cross between *csp* and *Solanum pimpinellifolium* LA1589 (TGRC accession number). The F_2 population was grown in an open field in Shunyi District, Beijing, China, during the spring and summer of 2020. The outcross seed number assay was performed using the tomato line Micro-Tom. The tomato cultivar Ailsa Craig (AC) was employed for the gene editing of the *TAP3* gene.

2.2. A Phenotypic Analysis of the csp Mutant

The morphology of the flowers of the WT and the *csp* mutant was observed at the anthesis stage using the methods that have been previously described [16]. The entire flower was photographed with a camera (Canon EOS 70D, Canon Inc., Tokyo, Japan). The anther cones and dissected stamens were observed using a stereomicroscope (Carl Zeiss Micro Imaging GmbH, Gottingen, Germany). Pollen viability was tested as described by Sinha and Rajam [29]. Pollen was collected from the WT and the *csp* mutant, stained with

2% aceto-carmine, and examined using a microscope (BX51, Olympus Corporation, Tokyo, Japan). Fruit set data were collected after self-pollination or outcrossing with Micro-Tom.

2.3. Molecular Marker Development and Genotyping

Insertions and deletions (InDels) were identified by comparing the sequences of tomato lines Heinz 1706 and LA1589, whose whole-genome sequences were published and released on the Sol Genomics Network (SGN, https://solgenomics.net/, accessed on 10 March 2024). PCR primers matching the flanking regions of these InDels were designed using the Primer-BLAST tool available from the National Center for Biotechnology Information (NCBI, http://www.ncbi.nlm.nih.gov/tools/primer-blast/). These primers were used to test the sequence polymorphisms between the *csp* mutant and LA1589. The *CSP* candidate gene-specific marker, csp-LTR, was developed based on the sequence alteration within the *CSP* candidate gene. General information about these markers can be found in Table S1. The PCR conditions were as follows: 94 °C for 3 min; followed by 35 cycles of 94 °C for 30 s, 52 °C for 30 s, and 72 °C for 30–60 s; and 72 °C for 5 min. The PCRs were performed on a PCR instrument (Bio-Rad, Hercules, CA, USA), and the PCR products of these markers were separated on a 3.0% agarose gel.

2.4. The Genetic Analysis and Fine Mapping of the csp Locus

The genetic analysis of the *csp* locus was performed using the Chi-square test on 270 plants of the F_2 population. For the preliminary mapping of the *csp* locus, 35 male sterile plants in the F_2 population were genotyped using the available markers in our research group. For the fine mapping of the *csp* locus, 1162 plants from the entire F_2 population were genotyped using InDel markers located between HP619 and HP621 (Table S1).

2.5. Candidate Gene Analysis

The putative genes in the region harboring the *csp* locus were identified by searching the tomato genome annotation database (ITAG release 4.0) on the SGN website. The candidate gene of *CSP* was amplified with the primers listed in Table S2 and sequenced at BGI TechSolutions Co., Ltd. (Beijing, China). To discover the structural variation in the *csp* mutant, it was re-sequenced at Beijing Biomarker Technologies Co., Ltd. (Beijing, China). The fragment containing the retrotransposon insertion in the *csp* mutant was amplified using 2× Phanta Max Master Mix (Dye Plus) (Cat. No. P525-03, Vazyme, Nanjing, China) and sequenced at BGI TechSolutions Co., Ltd. (Beijing, China) (see Tables S3 and S5).

2.6. RNA Extraction, cDNA Synthesis, and qPCR Analysis

The sepals, petals, stamens, and carpels of young flower buds measuring approximately 3–5 mm in length [30] were collected from the WT and the *csp* mutant and rapidly frozen in liquid nitrogen. Each tissue sample comprised three biological replicates, and each replicate contained samples from at least three plants. Total RNA was isolated using the RNA extraction kit (Cat. No. RP3401; Bioteke, Beijing, China), and cDNA was synthesized from 1 μg of total RNA using GoScript™ Reverse Transcriptase (Cat. No. A5003; Promega, Madison, WI, USA). The qPCR was performed using the methods previously described [31]. The primers for qPCR are provided in Table S4. The $2^{-\Delta\Delta CT}$ method was used to calculate relative gene expression, which was determined from qPCR experiments [32]. The data were analyzed using IBM SPSS Statistics 20.0 software, and a *t*-test was used to assess statistically significant differences.

2.7. CRISPR/cas9 Gene Editing Vector Construction, Plant Transformation, and Mutant Phenotypic Analysis

The CDS sequence of the *TAP3* gene was obtained from the SGN website. The candidate CRISPR/Cas9 (clustered regularly interspaced short palindromic repeats/CRISPR-associated protein 9) target sequence was identified using the website http://skl.scau.edu.cn/, accessed on 10 March 2024. Two sequences in the first exon of the *TAP3* gene Target-1

(AAGAAATGGGCTATTCAAGAAGG) and Target-2 (ATTGTTATGATTTCTAGTACTGG) were selected for the gene editing of *TAP3*. The two target sequences were ligated into the vector pMGET (Tables S5–S7), a vector for multi-gene editing made in our research group, to construct the vector pCSPDC [33]. The vector was then transferred into *Agrobacterium tumefaciens* (GV3101) using the freeze–thaw method. The agrobacterium mediated genetic transformation method was previously described by Van Eck [34].

Positive transgenic seedlings were identified using the primers Cas9-909F and Cas9-2450R (Table S5). The DNA fragments containing the *TAP3* target sites Target-1 and Target-2 were amplified with the primers CX-F and CX-R and ligated into a pEASY-Blunt Zero Cloning vector (pEASY-Blunt Zero Cloning Kit, Cat. No. CB501-02; TransGen Biotech, Beijing, China). Twelve single clones per PCR product were picked and sequenced at BGI TechSolutions Co., Ltd. (Beijing, China).

The T_0 generation gene-edited plants were grown in a greenhouse in Haidian District, Beijing, China. The morphology of the flowers and pollen was observed at anthesis using the methods that have been previously described [16]. For the allelism test, the homologous null mutant of the T_0 generation of the *TAP3* gene-edited line was crossed with *CSP/csp* heterozygous plants. Non-transgenic seedlings were chosen to be cultivated in a greenhouse located in the Haidian District of Beijing, China, in order to conduct a subsequent analysis of their phenotypic and genotypic characteristics.

3. Results

3.1. A Phenotypic Analysis of the csp Mutant

csp is a natural mutant that was found in a BIL in our research group. The flowers of the *csp* mutant exhibited sepaloid petals and carpelloid stamens (Figure 1b,d,f,g). Up to ninety-four percent of the stamens were completely transformed into carpels (Table 1), and all stamens did not produce pollen (Figure 1i). Some carpelloid stamens developed fruit-like organs, and most of the carpels produced seedless fruits when they were not pollinated (Figure 1k,m,o). Seeds could develop when the flowers of the *csp* mutant were manually crossed with wild-type pollen (Figure 1q). However, the number of seeds per fruit of the *csp* mutant was about one-third of that of the WT (Figure 1r).

Table 1. Proportion of stamens with different phenotypes in *csp* and WT.

Phenotypic Statistics	WT	*csp*
No. of observed stamens	228	198
Normal stamens (NOs)	228	0
Carpelloid structures (CSs)	0	0
Naked external ovules on the adaxial surface (EOs)	0	12 (6%)
Complete transformation into carpels (TC)	0	186 (94%)

3.2. A Genetic Analysis of the csp Locus

The F_1 plants derived from a cross between *csp* and LA1589 displayed normal stamens. A total of 270 plants from an F_2 population, which was derived from the above F_1 plants, were investigated on the phenotype of stamens. A total of 196 plants showed normal stamens, and 74 plants produced carpelloid stamens. This result was in agreement with the expected segregation ratio of 3:1 using the Chi-square test ($\chi^2 = 0.835$, less than χ^2 0.05 = 3.84), indicating that the *csp* phenotype was controlled by a single recessive gene.

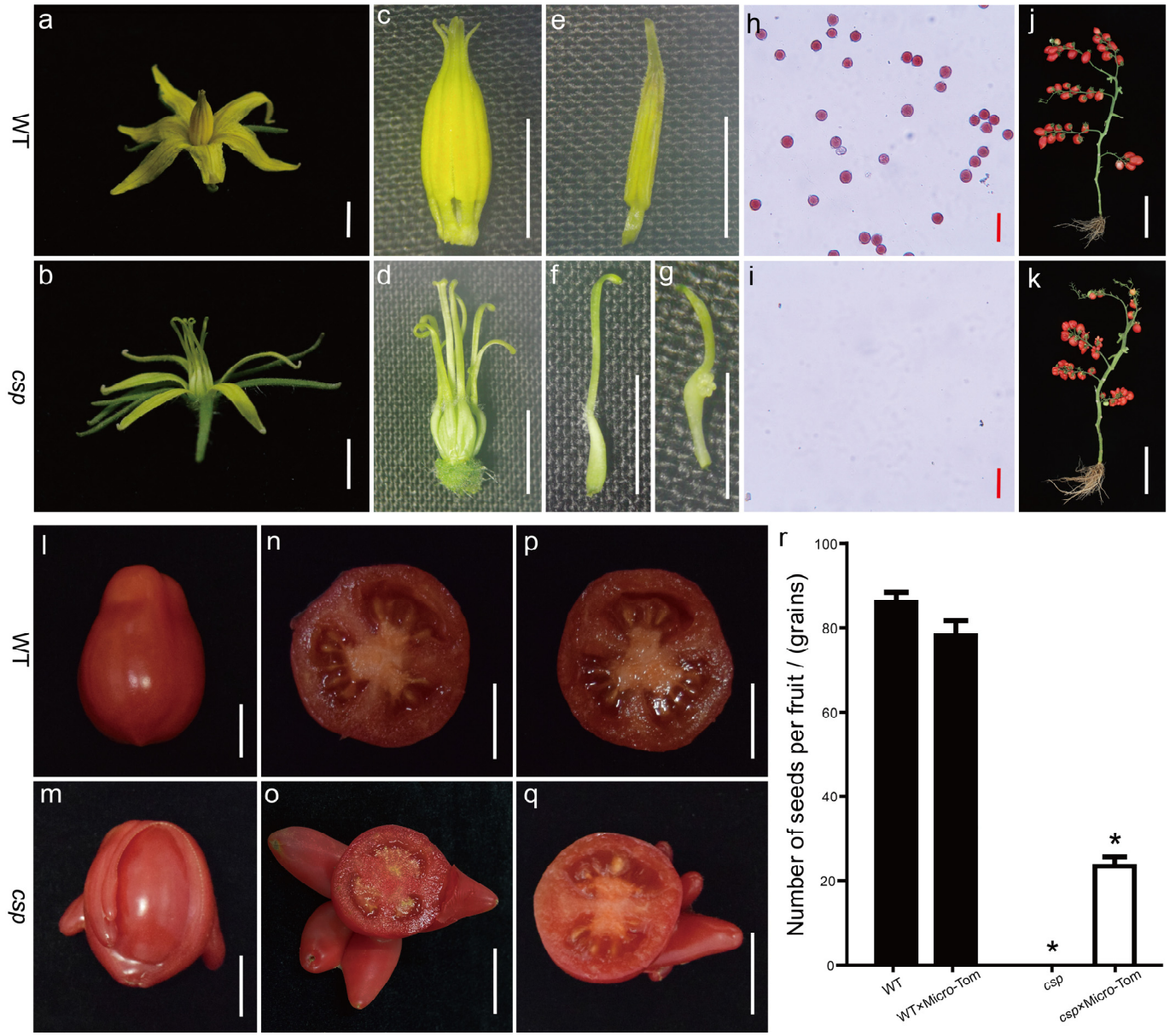

Figure 1. Phenotype of natural mutant *csp*. (**a**) WT flower; (**b**) *csp* flower; white bar is 1 cm. (**c**) WT anther cone; (**d**) *csp* anther cone; (**e**) WT stamen; (**f**) *csp* stamen completely transformed into carpel; (**g**) *csp* stamen with naked external ovules on adaxial surface; white bar is 0.5 cm. (**h**) WT pollen; (**i**) *csp* pollen; red bar is 50 μm. (**j**) Fruit setting of WT; (**k**) fruit setting of *csp*, white bar is 20 cm. (**l**) WT fruit; (**m**) *csp* fruit; (**n**) cross-section of WT self-pollinated fruit; (**o**) cross-section of *csp* self-pollinated fruit; (**p**) cross-section of WT outcrossed fruits; (**q**) cross-section of *csp* outcrossed fruits; white bar is 2 cm. (**r**) Seed number of self-pollinated fruits and outcrossed fruits with Micro-Tom. Asterisks indicate a signifcant diference (*, $p < 0.05$) between WT and *csp*; WT × Micro-Tom and *csp* × Micro-Tom.

3.3. The Fine Mapping of the csp Locus

For the preliminary mapping of the *csp* locus, 35 mutant plants from the F_2 population were genotyped using InDel markers on the chromosomes containing the B-class genes. This was conducted because the carpelloid stamens of the *csp* mutant were similar to the phenotype of B-class gene mutants. The results indicated that the *csp* locus was linked to the molecular markers on chromosome 4 that contained the *TAP3* gene. Furthermore, it was located within a 1.3 Mb region between the molecular markers HP619 and HP621 (Figure 2a).

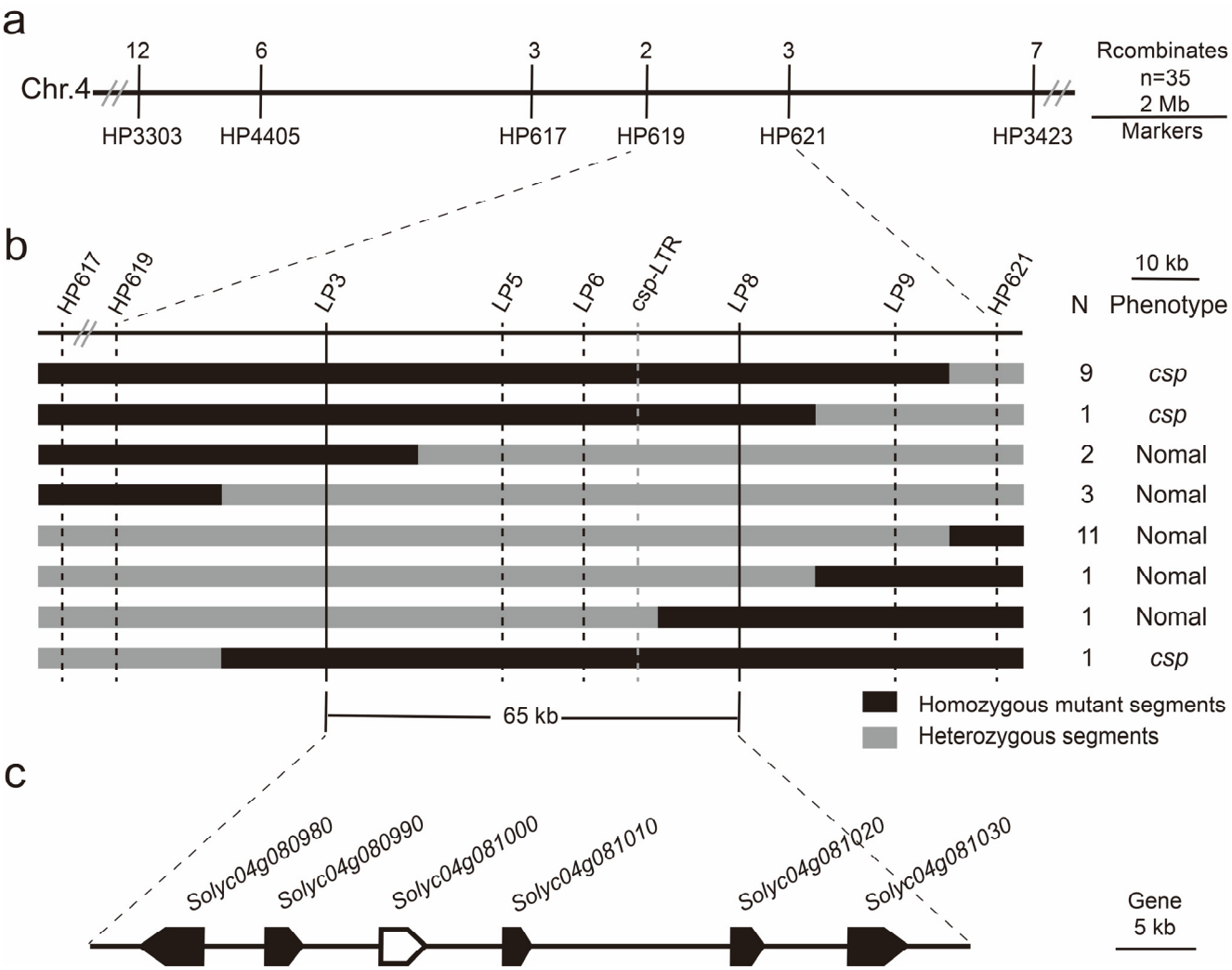

Figure 2. The fine mapping of the *csp* locus. (**a**) The preliminary mapping of the *csp* locus. n = 35 presents the first 35 mutant plants in the F_2 population; (**b**) the fine mapping of the *csp* locus, N represents the number of recombinants; the black box presents the mutant homozygous segments, and the gray box presents the heterozygous segments; (**c**) the predicted genes from ITAG release 4.0 in the region encompassing the *csp* locus. The arrows indicate the direction of the transcription of the predicted genes, and the white arrow presents the most likely candidate gene for *CSP*.

To fine map the *csp* locus, 1162 plants from the entire F_2 population were genotyped with markers HP619 and HP621. A total of 29 recombinants, which were determined to be homozygous for the *csp* mutant for only one of these two markers, were selected for further genotyping using an additional five markers (see Table S1). Subsequently, the *csp* locus was finally localized within a 65 kb interval flanked by markers LP3 and LP8 (Figure 2b).

3.4. Candidate Gene Analysis

Six predicted genes were identified in the 65 kb region containing the *csp* locus by searching the tomato genome annotation database (ITAG release 4.0) on the SGN website (Figure 2c, Table 2). Among them, *Solyc04g081000* encodes *TAP3* (syn. *SlDEF*, Table 2). A functional analysis of group B genes has shown that *TAP3* regulates the development of stamens and petals in the tomato [35]. Therefore, it is hypothesized that *TAP3* may be a candidate gene for *CSP*.

Table 2. Predict genes in the *csp* locus.

Gene	Position	Function
Solyc04g080980.2	SL4.0ch04: 63,014,916. . .63,020,499 (−)	Coatomer subunit alpha
Solyc04g080990.2	SL4.0ch04: 63,025,202. . .63,027,315 (+)	S-type anion channel *SLAH1*
Solyc04g081000.3	**SL4.0ch04: 63,032,681. . .63,036,255 (+)**	***TAP3*, Tomato locus *SlDEF* (Deficiens), MADS box transcription factor**
Solyc04g081010.2	SL4.0ch04: 63,041,514. . .63,042,316 (+)	Unknown protein
Solyc04g081020.3	SL4.0ch04: 63,056,424. . .63,057,867 (+)	B-box zinc finger protein 24
Solyc04g081030.3	SL4.0ch04: 63,064,187. . .63,069,499 (+)	Protein disulfide-isomerase 5-3

To discover sequence alteration within the *TAP3* gene in the *csp* mutant, six pairs of primers (Table S2) were designed according to its full-length genomic sequence in the tomato reference genome (version SL4.0). PCR was performed using these primers, and a band was not amplified with the second pair of primers (LS2) in the *csp* mutant, but it was amplified in the WT (Figure 3a). The PCR bands amplified with the other five pairs of primers were sequenced (Figure 3a), and no sequence polymorphism was found between the *csp* mutant and the WT. An analysis of the re-sequencing data revealed a potential transposon insertion in the *TAP3* gene of the *csp* mutant at position SL4.0ch04: 63,033,062 (Figure 3b). This conclusion was drawn based on the observation that the sequence of the paired reads of some reads near SL4.0ch04: 63,033,062 in the *csp* mutant appeared to be derived from transposable elements (TEs). To confirm this finding, a pair of primers was designed around SL4.0ch04: 63,033,062 for the PCR amplification of the long strand. The WT and the *csp* mutant produced bands of approximately 800 bp and 5 kb, respectively (Figure 3c). The 5 kb PCR band was then ligated into a blunt-zero vector and sequenced. The sequencing results indicated that a *copia* long terminal repeat (LTR) retrotransposon [36] was inserted in the first intron of the *TAP3* gene of the *csp* mutant (Figure 3d and Figure S1). This insertion may lead to a loss-of-function of the *TAP3* gene.

Based on the sequence of the retrotransposon inserted in the *TAP3* gene of the *csp* mutant, an InDel marker named csp-LTR was developed in this study (Figure 3d). This marker could accurately distinguish the *csp* mutant, homozygous WT (*CSP*/*CSP*), and heterozygous plants (*CSP*/*csp*) (Figure 3e).

3.5. Expression Analysis of Floral Organ Identity Genes, Pollen Development Marker Genes, and Pistil-Specific Genes

Given that the *csp* mutant contained an insertion in the B-class gene *TAP3* and displayed carpelloid stamens (Figures 1 and 3d), the transcriptional expression of *TAP3* and the other floral organ identity genes, as well as the marker genes of pollen and pistil development, was examined in the *csp* mutant and the WT. The B-class genes *TAP3* and *SlGLO2* were significantly down-regulated in the stamens of the *csp* mutant. However, there was no significant difference in the expression of B-class genes *TM6* and *SlGLO1* between the stamens of the *csp* mutant and the WT. The C-class gene *TAG1* was significantly down-regulated in stamens, while the E-class gene *TM5* was significantly up-regulated in petals (Figure 4). The pollen development marker gene *Aspartic proteinase* was significantly down-regulated in the stamens of the *csp* mutant. In contrast, the pistil-specific gene *SITTS* was significantly up-regulated in both the stamens and pistils of the *csp* mutant.

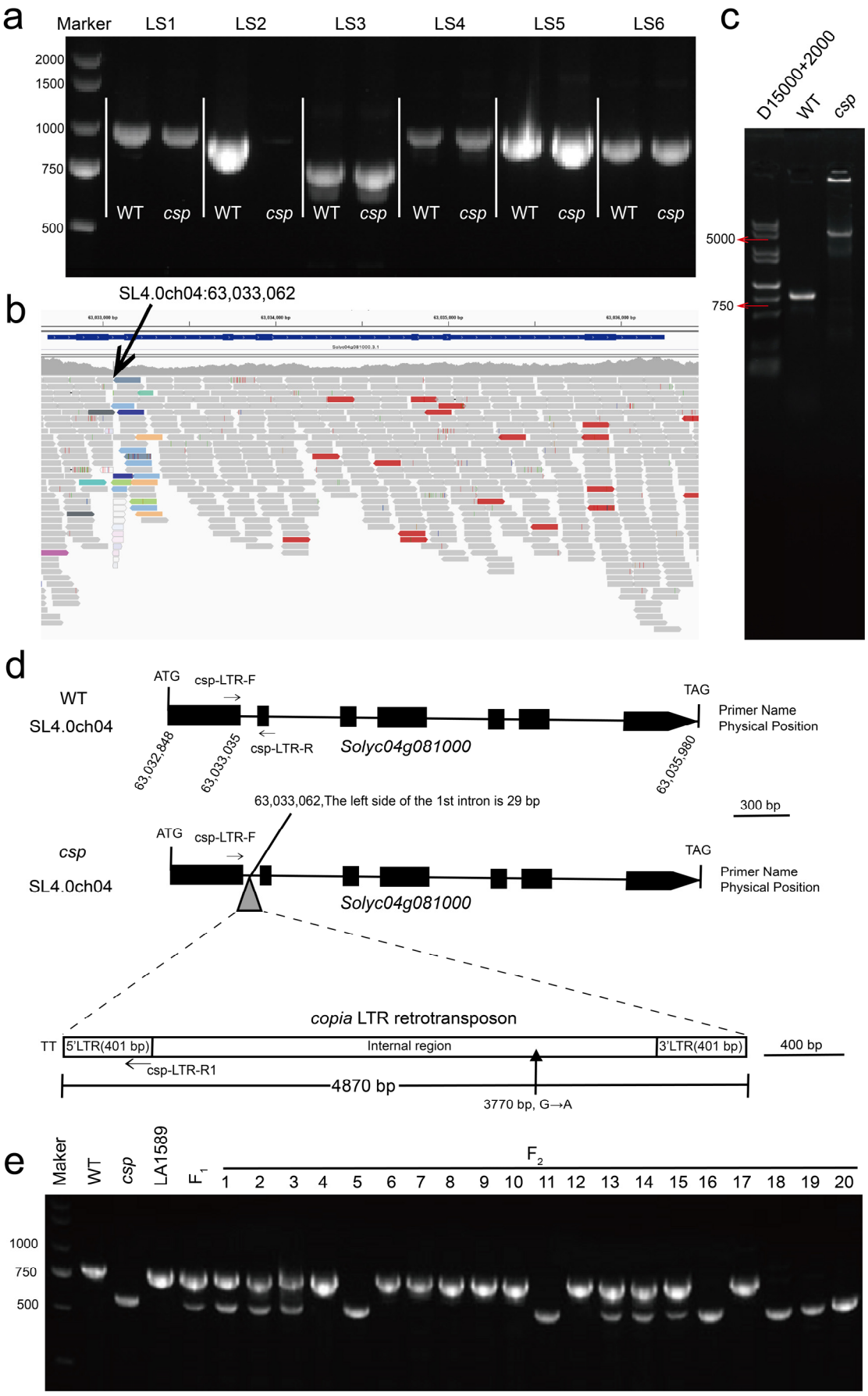

Figure 3. The structural variation in the *TAP3* gene of the *csp* mutant. (**a**) The agarose gel electrophoresis of PCR fragments amplified from both the WT and the *csp* mutant using primers specific to the *TAP3*

gene. (**b**) The browser displayed that the re-sequencing reads of the *csp* mutant were aligned to the Heinz 1706 reference genome assembly. (**c**) The agarose gel electrophoresis of PCR fragments amplified from both the WT and the *csp* mutant using the primers located around the insertion site. (**d**) The sequence polymorphism of the *TAP3* gene in the *csp* mutant. Black squares and black lines represent the exons and introns of *Solyc04g081000*, respectively. The gray triangle represents the insertion of the CopiaSL-37 retrotransposon. csp-LTR-F, csp-LTR-R, and csp-LTR-R1 are the primers used in generating the csp-LTR marker, and arrows indicate the position and direction of these primers. (**e**) The agarose gel electrophoresis of PCR fragments amplified from the WT, LA1589, *csp*, F_1, and F_2 plants using the csp-LTR marker.

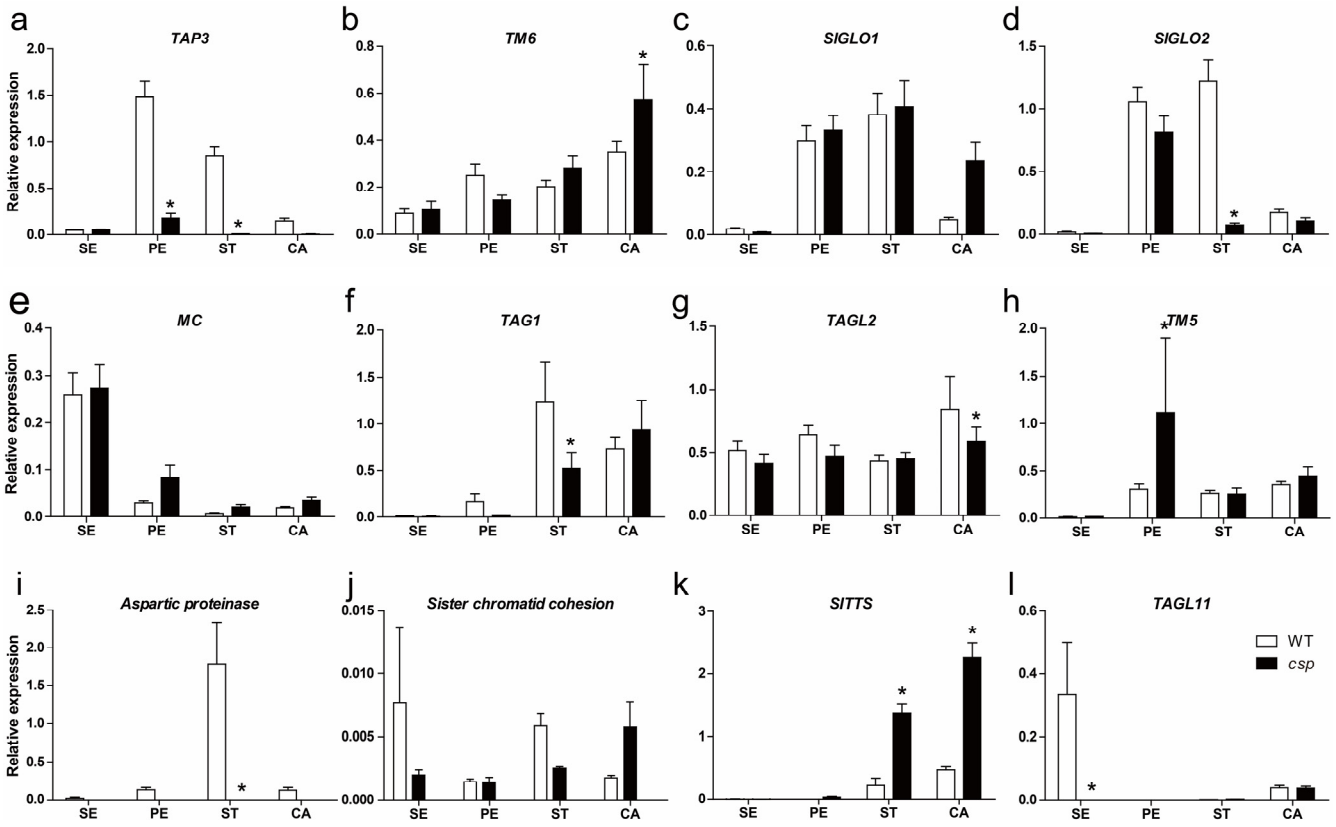

Figure 4. An expression analysis of the genes related to floral organ identity, pollen, and pistil development in flower buds in the *csp* mutant and the WT. (**a**) *TAP3*; (**b**) *TM6*; (**c**) *SlGLO2*; (**d**) *SlGLO1*; (**e**) *MC*; (**f**) *TAG1*; (**g**) *TAGL2*; (**h**) *TM5*; (**i**) *Aspartic proteinase*; (**j**) *Sister chromatid cohesion*; (**k**) *SlTTS*; (**l**) *TAGL11*; the experimental data were subjected to a *t*-test, and a significance level of $p < 0.05$ was considered significant. An asterisk (*) indicated significant differences in gene expression. The floral organs were labeled as follows: SE for sepals, PE for petals, ST for stamens, and CA for carpels.

3.6. Validation of Candidate Gene by Gene Editing and Allelism Test

The *TAP3* gene was knocked out using CRISPR-Cas9 technology (Figure 5a). Twelve T_0 plants contained mutations in the *TAP3* gene, and most of these mutations were chimeric and multiple allelic (Figure S2). Three T_0 plants, AT−4 (also named *tap3*^{cr4}), AT−5, and AT−23, were selected for phenotypic observation. AT−4 and AT−5 were null mutants of the *TAP3* gene (Figure 5b). They exhibited sepaloid petals and carpelloid stamens and produced seedless fruits, which were similar to the *csp* mutant (Figure 5). AT−23 was heterozygous (Figure 5b). It looked as normal as the WT (Figure 5). An allelism test showed that *tap3*^{cr4} is allelic to *csp* (Figure S3). These results indicate that *csp* is a novel mutation of the *TAP3* gene.

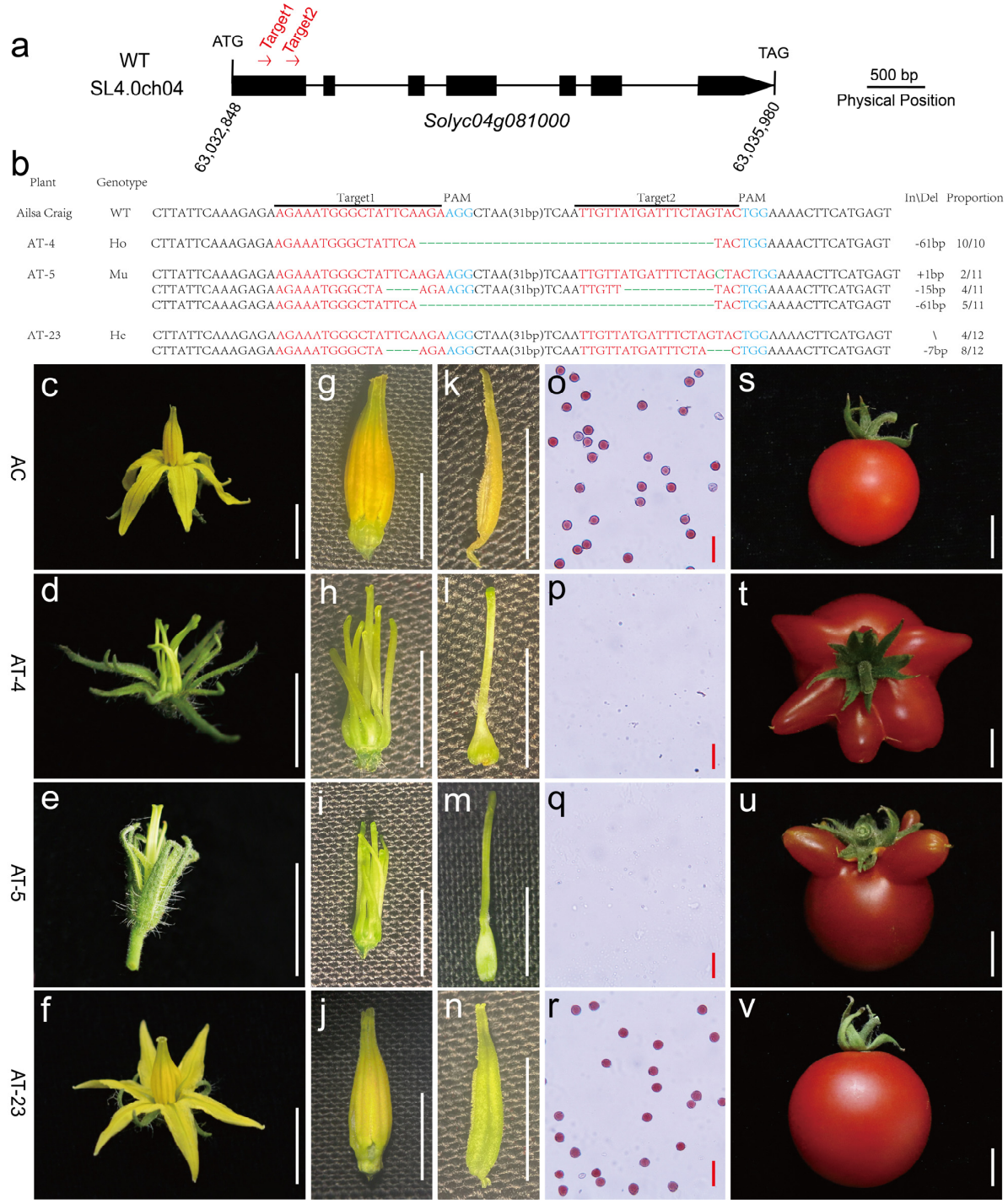

Figure 5. CRISPR/Cas9-engineered mutations and phenotypes of the *tap3*^{cr} mutants. (**a**) A schematic illustration of the two targeting sequences (red arrows) of *TAP3* (*Solyc04g081000*). (**b**) *tap3*^{cr} mutant alleles identified from three T_0 plants. WT represents the wild type, Ho represents the homozygous mutation, Mu represents the multi-allele mutation, and He represents the heterozygous mutation. The red letters represent the target sequence of the *TAP3* gene, the blue letters indicate the protospacer-adjacent motif (PAM), the green letter indicates the insertion sequence, and the green hyphens mark the deletion sequences. The number on the right indicates the number of bases inserted or deleted. A flower of AC (**c**), AT−4 (**d**), AT−5 (**e**), and AT−23 (**f**). The white bar is 1 cm. An anther cone of AC (**g**), AT−4 (**h**), AT−5 (**i**), and AT−23 (**j**). The white bar is 0.5 cm. Stamens of AC (**k**), AT−4 (**l**), AT−5 (**m**), and AT−23 (**n**). The white bar is 0.5 cm. Pollens of AC (**o**), AT−4 (**p**), AT−5 (**q**), and AT−23 (**r**). The red bar is 50 μm. Fruits of AC (**s**), AT−4 (**t**), AT−5 (**u**), and AT−23 (**v**). The white bar is 1 cm.

4. Discussion

Male sterility and parthenocarpy are two attractive traits in tomato breeding [37,38]. The stamen carpelloid mutant usually displays male sterility [8]. The genes underlying some carpelloid stamen mutants or parthenocarpic fruit mutants have been cloned, but many are still unknown. Carpelloid stamens and parthenocarpy usually occur independently. Our group found a natural mutant, *csp*, whose phenotype differed to some extent from the reported tomato B-class gene mutants. The *csp* mutant showed stronger stamen deformities compared to *ms-15*, *ms-26*, *ms-30*, *ms-33*, *ms-47*, *7B-1*, and *sl-2*, as it had a higher percentage of stamens completely transformed into carpels [11,16,17]. Additionally, *csp* may also have a higher percentage of parthenocarpic fruits compared to the loss-of-function mutants of the tomato B-class gene (Figure 1, Table 1). However, the petals of *csp* only exhibited slight transformation into petals, whereas the petals of *sl-Pr* and *tap3* were completely transformed into sepals [13–15]. The *csp* locus was fine mapped to a 65 kb interval that contained six putative genes (Figure 2b, Table 2). Thereinto, *Solyc04g081000* encodes the tomato class B MADS box gene *TAP3* (Figure 2c, Table 2). A sequencing data analysis showed that a retrotransposon of approximately 5 kb was inserted in the first intron of the *TAP3* gene of the *csp* mutant (Figure 3), resulting in an almost absent expression of the *TAP3* gene in petals and stamens of the *csp* mutant (Figure 4). A phenotypic analysis of the *TAP3* gene-edited mutants (Figure 5) and an allelism test (Figure S3) indicated that *TAP3* was the gene underlying the *csp* mutant. *TAP3* has been reported to be the gene responsible for *sl-Pr* and *sl-LA0269* [13]. This means that *csp* was a novel allele of the *TAP3* gene. The reason for the different phenotype of these mutants needs further study.

Tomato possesses four B-class genes, namely *TAP3*, *TM6*, *SlGLO1*, and *SlGLO2* (*TPI*). *TAP3* and *TM6* are identified as duplicate orthologs, as are *SlGLO1* and *SlGLO2* (*TPI*). These genes are known to play conserved roles in determining petal and stamen identities while also undergoing subfunctionalization [10,39]. Notably, they exhibit distinct expression patterns within floral organs. Specifically, *TAP3*, *SlGLO1*, and *SlGLO2* (*TPI*) are found to be expressed predominantly in petals and stamens, whereas *TM6* shows high expression levels in petals, stamens, and carpels, as illustrated in Figure 4 of this study and previous research [11,17,39]. The mutants of the four B-class genes exhibit varying effects on the expression of floral identity genes. Specifically, in the *TM6* gene mutant *ms-15*^{26}, all four B-class genes and one C-class gene *TAG1* show down-regulation in stamens [11]. In the *SlGLO2* (*TPI*) gene mutant *ms-30*, three B-class genes (*SlGLO2* (*TPI*), *TAP3*, *SlGLO1*), one C-class gene *TAG1*, and one E-class gene *TAGL2* are down-regulated in stamens [17]. Conversely, in *SlGLO1* RNAi lines, *TM6*, *TAG1*, and the E-class gene *TM5* exhibit up-regulation in stamens [39]. Furthermore, in the *TAP3* gene mutant *csp*, *TAP3*, *SlGLO2* (*TPI*), and *TAG1* are down-regulated in stamens, as shown in Figure 4 of this study. The mutants of each of the B-class genes in tomato exhibit distinct phenotypes. Specifically, mutants of *TM6* and *SlGLO2* (*TPI*) genes predominantly display carpelloid stamens and male sterility [11,17], whereas mutants of the *TAP3* gene exhibit sepalloid petals, carpelloid stamens, male sterility, and parthenocarpy (Figures 1 and 5) [14,15]. Further investigation is required to elucidate the molecular mechanisms underlying the subfunctionalization of the B-class genes in tomato.

TEs are important sources of phenotypic variation and evolution in plants [40–42]. Approximately two-thirds of the tomato genome is composed of TE sequences [43,44]. The tomato reference genome (*Solanum lycopersocum* cv. Heinz 1706, release SL2.5) contains 665,122 annotated TE sequences belonging to 818 families [43]. Domínguez et al. identified 6906 TE insertion polymorphisms (TIPs) from 602 cultivated and wild tomato accessions. They also identified at least 40 TIPs robustly that are associated with extreme variation in major agronomic traits or secondary metabolites using genome-wide association studies (GWASs) [45]. Several studies have also revealed that tomato phenotypic variations or mutants result from the insertion of TEs [23]. In this study, a part of the *TAP3* gene could not be amplified from the *csp* mutant using normal elongation time (Figure 4a). Through paired-end whole-genome re-sequencing data analysis and long PCR amplification, an

approximately 5 kb long terminal sequence repeat retrotransposon, CopiaSL-37 (LTR retrotransposon CopiaSL-37), was found in the first intron of the *TAP3* gene in the *csp* mutant (Figure 3d). This resulted in an almost absent expression of the *TAP3* gene in the petals and stamens of the *csp* mutant (Figure 4a). It was hypothesized that *7B-1* and *sl-2* contained a structural variation in the *SlGLO2* gene [16]. Recently, a retrotransposon of approximately 4.8 kb was found in the *SlGLO2* gene in the *7B-1* and *sl-2* mutant through long PCR amplification in our group [17]. Therefore, long PCR amplification might be tried first when a hypothesized structural variation needs to be revealed, because TEs are known to be one of the major sources of structural variations [43,44].

Supplementary Materials: The following supporting information can be downloaded at https://www.mdpi.com/article/10.3390/horticulturae10040403/s1, Figure S1: The sequence of the *copia* LTR retrotransposon in the *csp* mutant; Figure S2: Sequence variations of the *TAP3* gene-edited T_0 generation plants; Figure S3: An allelism test between the *csp* mutant and *TAP3* gene-edited mutant $tap3^{cr4}$; Table S1: General information of InDel markers for mapping *CSP*; Table S2: General information of primers for amplification and sequencing of *TAP3* gene; Table S3: The primers for sequencing the *copia* LTR retrotransposon in the *csp* mutant; Table S4: The primers used in real-time PCR; Table S5: The primers for CRISPR/Cas9 gene editing; Table S6: PCR amplification system; Table S7: Golden Gate reactions system.

Author Contributions: Conceptualization, X.W., Y.G., L.L., X.L., C.Z., Y.D., J.L. and Z.H.; methodology, S.L., K.W. and Z.H.; validation, formal analysis, investigation, and data curation, S.L., K.W., L.Z., Y.N., F.L. and Z.H.; writing—original draft preparation, S.L.; writing—review and editing, S.L., K.W., L.Z. and Z.H.; visualization, S.L.; supervision, X.W., Y.G., L.L., X.L., C.Z., Y.D., J.L. and Z.H.; project administration, Z.H.; funding acquisition, X.W. and Z.H. All authors have read and agreed to the published version of the manuscript.

Funding: This work was supported by grants from the National Key Research and Development Program of China (No. 2022YFD1200500), the National Natural Science Foundation of China (Nos. 31872949 and 31672154), and the China Agriculture Research System (No. CARS-23-A06).

Data Availability Statement: Data are contained within the article and Supplementary Materials.

Conflicts of Interest: The authors declare no conflicts of interest.

References

1. Shu, J.; Liu, Y.; Li, Z.; Zhang, L.; Fang, Z.; Yang, L.; Zhuang, M.; Zhang, Y.; Lv, H. Organelle simple sequence repeat markers help to distinguish carpelloid stamen and normal cytoplasmic male sterile sources in Broccoli. *PLoS ONE* **2015**, *10*, e0138750. [CrossRef] [PubMed]
2. Kramer, E.M.; Dorit, R.L.; Irish, V.F. Molecular evolution of genes controlling petal and stamen development: Duplication and divergence within the *APETALA3* and *PISTILLATA* MADS-box gene lineages. *Genetics* **1998**, *149*, 765–783. [CrossRef]
3. Jack, T. Relearning our ABCs: New twists on an old model. *Trends Plant Sci.* **2001**, *6*, 310–316. [CrossRef] [PubMed]
4. Kim, S.; Yoo, M.J.; Albert, V.A.; Farris, J.S.; Soltis, P.S.; Soltis, D.E. Phylogeny and diversification of B-function MADS-box genes in angiosperms: Evolutionary and functional implications of a 260-million-year-old duplication. *Am. J. Bot.* **2004**, *91*, 2102–2118. [CrossRef]
5. Murai, K.; Takumi, S.; Koga, H.; Ogihara, Y. Pistillody, homeotic transformation of stamens into pistil-like structures, caused by nuclear-cytoplasm interaction in wheat. *Plant J.* **2002**, *29*, 169–181. [CrossRef]
6. Kang, L.; Li, P.; Wang, A.; Ge, X.; Li, Z. A novel cytoplasmic male sterility in *Brassica napus* (inap CMS) with carpelloid stamens via protoplast fusion with Chinese woad. *Front. Plant Sci.* **2017**, *8*, 529. [CrossRef]
7. Wang, A.; Kang, L.; Yang, G.; Li, Z. Transcriptomic and iTRAQ-Based quantitative proteomic analyses of inap CMS in *Brassica napus* L. *Plants* **2022**, *11*, 2460. [CrossRef] [PubMed]
8. Pucci, A. *Characterization of Tomato (Solanum lycopersicum L.) Male Sterile Mutants Putatively Affected in Class B MADS-Box Transcription Factors*; Università Degli Studi Della Tuscia—Viterbo: Viterbo, Italy, 2015; Available online: http://hdl.handle.net/2067/2946 (accessed on 10 March 2024).
9. Weigel, D.; Meyerowitz, E.M. The ABCs of floral homeotic genes. *Cell* **1994**, *78*, 203–209. [CrossRef]
10. Geuten, K.; Irish, V. Hidden variability of floral homeotic B Genes in solanaceae provides a molecular basis for the evolution of novel functions. *Plant Cell* **2010**, *22*, 2562–2578. [CrossRef]
11. Cao, X.; Liu, X.; Wang, X.; Yang, M.; van Giang, T.; Wang, J.; Liu, X.; Sun, S.; Wei, K.; Wang, X.; et al. B-class MADS-box *TM6* is a candidate gene for tomato *male sterile-15*^{26}. *Theor. Appl. Genet.* **2019**, *132*, 2125–2135. [CrossRef]

12. Fonseca, R.; Capel, C.; Lebrón, R.; Ortiz-Atienza, A.; Yuste-Lisbona, F.J.; Angosto, T.; Capel, J.; Lozano, R. Insights into the functional role of tomato *TM6* as transcriptional regulator of flower development. *Hortic. Res.* **2024**, *11*, uhae019. [CrossRef] [PubMed]
13. Quinet, M.; Bataille, G.; Dobrev, P.I.; Capel, C.; Gómez, P.; Capel, J.; Lutts, S.; Motyka, V.; Angosto, T.; Lozano, R. Transcriptional and hormonal regulation of petal and stamen development by *STAMENLESS*, the tomato (*Solanum lycopersicum* L.) orthologue to the B-class *APETALA3* gene. *J. Exp. Bot.* **2014**, *65*, 2243–2256. [CrossRef]
14. De Martino, G.; Pan, I.; Emmanuel, E.; Levy, A.; Irish, V.F. Functional analyses of two tomato *APETALA3* genes demonstrate diversification in their roles in regulating floral development. *Plant Cell* **2006**, *18*, 1833–1845. [CrossRef]
15. Okabe, Y.; Yamaoka, T.; Ariizumi, T.; Ushijima, K.; Kojima, M.; Takebayashi, Y.; Sakakibara, H.; Kusano, M.; Shinozaki, Y.; Pulungan, S.I.; et al. Aberrant stamen development is associated with parthenocarpic fruit set through up-regulation of gibberellin biosynthesis in tomato. *Plant Cell Physiol.* **2018**, *60*, 38–51. [CrossRef]
16. Pucci, A.; Picarella, M.E.; Mazzucato, A. Phenotypic, genetic and molecular characterization of *7B-1*, a conditional male-sterile mutant in tomato. *Theor. Appl. Genet.* **2017**, *130*, 2361–2374. [CrossRef] [PubMed]
17. Wei, K.; Li, X.; Cao, X.; Li, S.; Zhang, L.; Lu, F.; Liu, C.; Guo, Y.; Liu, L.; Zhu, C.; et al. Candidate gene identification and transcriptome analysis of tomato *male sterile-30* and functional marker development for *ms-30* and its alleles, *ms-33*, *7B-1*, and *stamenless-2*. *Int. J. Mol. Sci.* **2024**, *25*, 3331. [CrossRef]
18. Fayaz, Z.; Nazir, G.; Masoodi, U.; Afroza, B.; Asma, S.; Rashid, M. Parthenocarpy: "A potential trait to exploit in vegetable crops". *Environ. Ecol.* **2021**, *39*, 1332–1346.
19. Sharif, R.; Su, L.; Chen, X.; Qi, X. Hormonal interactions underlying parthenocarpic fruit formation in horticultural crops. *Hortic. Res.* **2022**, *9*, uhab024. [CrossRef]
20. Beraldi, D.; Picarella, M.E.; Soressi, G.P.; Mazzucato, A. Fine mapping of the *parthenocarpic fruit* (*pat*) mutation in tomato. *Theor. Appl. Genet.* **2004**, *108*, 209–216. [CrossRef] [PubMed]
21. Selleri, L. *Positional Cloning of the Parthenocarpic Fruit (Pat) Mutant Gene and Identification of New Parthenocarpic Sources in Tomato (Solanum lycopersicum,* L.*)*; Università Degli Studi Della Tuscia—Viterbo: Viterbo, Italy, 2011.
22. Nunome, T. Map-based cloning of tomato parthenocarpic pat-2 gene. *J-STAGE* **2016**, *51*, 37–40. [CrossRef]
23. Takisawa, R.; Nakazaki, T.; Nunome, T.; Fukuoka, H.; Kataoka, K.; Saito, H.; Habu, T.; Kitajima, A. The parthenocarpic gene *Pat-k* is generated by a natural mutation of *SlAGL6* affecting fruit development in tomato (*Solanum lycopersicum* L.). *BMC Plant Biol.* **2018**, *18*, 72. [CrossRef] [PubMed]
24. Klap, C.; Yeshayahou, E.; Bolger, A.M.; Arazi, T.; Gupta, S.K.; Shabtai, S.; Usadel, B.; Salts, Y.; Barg, R. Tomato facultative parthenocarpy results from *SlAGAMOUS-LIKE 6* loss of function. *Plant Biotechnol. J.* **2017**, *15*, 634–647. [CrossRef]
25. Bassel, G.W.; Mullen, R.T.; Bewley, J.D. *procera* is a putative DELLA mutant in tomato (*Solanum lycopersicum*): Effects on the seed and vegetative plant. *J. Exp. Bot.* **2008**, *59*, 585–593. [CrossRef]
26. Saito, T.; Ariizumi, T.; Okabe, Y.; Asamizu, E.; Hiwasa-Tanase, K.; Fukuda, N.; Mizoguchi, T.; Yamazaki, Y.; Aoki, K.; Ezura, H. Tomatoma: A novel tomato mutant database distributing micro-tom mutant collections. *Plant Cell Physiol.* **2011**, *52*, 283–296. [CrossRef] [PubMed]
27. Mazzucato, A.; Cellini, F.; Bouzayen, M.; Zouine, M.; Mila, I.; Minoia, S.; Petrozza, A.; Picarella, M.E.; Ruiu, F.; Carriero, F. A TILLING allele of the tomato *Aux/IAA9* gene offers new insights into fruit set mechanisms and perspectives for breeding seedless tomatoes. *Mol. Breed.* **2015**, *35*, 22. [CrossRef]
28. Mazzucato, A.; Taddei, A.R.; Soressi, G.P. The *parthenocarpic fruit* (*pat*) mutant of tomato (*Lycopersicon esculentum* Mill.) sets seedless fruits and has aberrant anther and ovule development. *Development* **1998**, *125*, 107–114. [CrossRef] [PubMed]
29. Sinha, R.; Rajam, M.V. RNAi silencing of three homologues of *S-adenosylmethionine decarboxylase* gene in tapetal tissue of tomato results in male sterility. *Plant Mol. Biol.* **2013**, *82*, 169–180. [CrossRef] [PubMed]
30. Brukhin, V.; Hernould, M.; Gonzalez, N.; Chevalier, C.; Mouras, A. Flower development schedule in tomato *Lycopersicon esculentum* cv. sweet cherry. *Sex. Plant Reprod.* **2003**, *15*, 311–320. [CrossRef]
31. Cao, X.; Qiu, Z.; Wang, X.; Van Giang, T.; Liu, X.; Wang, J.; Wang, X.; Gao, J.; Guo, Y.; Du, Y.; et al. A putative *R3 MYB* repressor is the candidate gene underlying *atroviolacium*, a locus for anthocyanin pigmentation in tomato fruit. *J. Exp. Bot.* **2017**, *68*, 5745–5758. [CrossRef]
32. Livak, K.J.; Schmittgen, T.D. Analysis of relative gene expression data using Real-Time quantitative PCR and the $2^{-\Delta\Delta CT}$ method. *Methods* **2001**, *25*, 402–408. [CrossRef] [PubMed]
33. Yang, M.X.; Liu, X.L.; Cao, C.; Wei, K.; Ning, Y.; Yang, P.; Li, S.S.; Chen, Z.Y.; Wang, X.X.; Guo, Y.M.; et al. Construction and application of a CRISPR/Cas9 system for multiplex gene editing in tomato. *Acta Hortic. Sin.* **2023**, *50*, 1215–1229. (In Chinese)
34. Van Eck, J.; Keen, P.; Tjahjadi, M. *Agrobacterium tumefaciens*-mediated transformation of tomato. *Methods Mol. Biol.* **2019**, *1864*, 225–234. [CrossRef]
35. Vekemans, D.; Viaene, T.; Caris, P.; Geuten, K. Transference of function shapes organ identity in the dove tree inflorescence. *New Phytol.* **2012**, *193*, 216–228. [CrossRef]
36. Paz, R.C.; Kozaczek, M.E.; Rosli, H.G.; Andino, N.P.; Sanchez-Puerta, M.V. Diversity, distribution and dynamics of full-length Copia and Gypsy LTR retroelements in *Solanum lycopersicum*. *Genetica* **2017**, *145*, 417–430. [CrossRef] [PubMed]
37. Medina, M.; Roque, E.; Pineda, B.; Cañas, L.; Rodriguez-Concepción, M.; Beltrán, J.P.; Gómez-Mena, C. Early anther ablation triggers parthenocarpic fruit development in tomato. *Plant Biotechnol. J.* **2013**, *11*, 770–779. [CrossRef] [PubMed]

38. Roque, E.; Gómez-Mena, C.; Hamza, R.; Beltrán, J.P.; Cañas, L.A. Engineered male sterility by early anther ablation using the pea anther-specific promoter PsEND1. *Front. Plant Sci.* **2019**, *10*, 819. [CrossRef]
39. Guo, X.; Hu, Z.; Yin, W.; Yu, X.; Zhu, Z.; Zhang, J.; Chen, G. The tomato floral homeotic protein *FBP1-like* gene, *SlGLO1*, plays key roles in petal and stamen development. *Sci. Rep.* **2016**, *6*, 20454. [CrossRef]
40. Alseekh, S.; Scossa, F.; Fernie, A.R. Mobile transposable elements shape plant genome diversity. *Trends Plant Sci.* **2020**, *25*, 1062–1064. [CrossRef]
41. Catlin, N.S.; Josephs, E.B. The important contribution of transposable elements to phenotypic variation and evolution. *Curr. Opin. Plant Biol.* **2022**, *65*, 102140. [CrossRef] [PubMed]
42. Pulido, M.; Casacuberta, J.M. Transposable element evolution in plant genome ecosystems. *Curr. Opin. Plant Biol.* **2023**, *75*, 102418. [CrossRef] [PubMed]
43. Jouffroy, O.; Saha, S.; Mueller, L.; Quesneville, H.; Maumus, F. Comprehensive repeatome annotation reveals strong potential impact of repetitive elements on tomato ripening. *BMC Genom.* **2016**, *17*, 624. [CrossRef] [PubMed]
44. Li, N.; He, Q.; Wang, J.; Wang, B.; Zhao, J.; Huang, S.; Yang, T.; Tang, Y.; Yang, S.; Aisimutuola, P.; et al. Super-pangenome analyses highlight genomic diversity and structural variation across wild and cultivated tomato species. *Nat. Genet.* **2023**, *55*, 852–860. [CrossRef] [PubMed]
45. Domínguez, M.; Dugas, E.; Benchouaia, M.; Leduque, B.; Jiménez-Gómez, J.M.; Colot, V.; Quadrana, L. The impact of transposable elements on tomato diversity. *Nat. Commun.* **2020**, *11*, 4058. [CrossRef] [PubMed]